Chapter 5

ENGINEERING ELECTRONIC STRUCTURE

Advanced devices place strong demands on semiconductor properties. To obtain the highest performance it is necessary to engineer the properties of constituent materials. In some devices, this means designing the electronic energy band structures. In other cases, the natures of defects in the materials are most critical. In this and the following chapter we consider band engineering and leave defect design to Chapter 7.

In Chapter 2, we discussed the basic physics that determines the electronic structure of a periodic solid. Now we will put some of that understanding to work. In this chapter we will further develop the physics underlying trends in semiconductor bands as a function of the atomic electronic states from which they are constructed. From this we will see how controlled modification of the chemistry and structure of a semiconductor can be used to engineer its energy bands. We will also step back and see how trends in real energy bands can be found, understood, and exploited to control energy gaps, energy-momentum relationships, and band edge energies. Chapter 2 gives an idea of why bands of states form and the breadth of a band of states between energy gaps for given configurations of atoms. It does not provide any specifics as to why one material is different from another, nor does it suggest why bands of states exhibit behaviors such as indirect energy gaps. Here we will examine the chemical basis for the observed variability.

The objective of this chapter is to provide an insight into the results of quantum-mechanical band structure calculations without relying on quantum mechanics itself in detail. The following assumes that the

majority of readers of this book will not have studied quantum mechanics beyond the brief review provided in Chapter 2. Details of the calculations of real band structures are therefore beyond the scope of this text. However, excellent, if more complex, explanations can be found in the classic texts *Solid State Physics*, by Ashcroft and Mermin, in more detail yet in *Electronic Structure* by Harrison, and in many other resources. Here we focus on the bigger picture of how solids organize their electrons. We will explore the functionalities of the bonding process and see how behaviors such as the common cation and common anion rules for heterojunctions arise, why energy band gaps decrease as the average size of a lattice increases, and many other typical behaviors.

5.1 LINKING ATOMIC ORBITALS TO BANDS

The quantum mechanics of bonding traces the evolution of the energies and distributions of electrons as atoms come together to form a solid. During this process, the states the electrons occupy develop from initial atomic orbitals to the energy bands of Chapter 2. The solutions of the Schrödinger Equation in the completed solid are constructed typically as a linear combination of the atomic orbitals (LCAO) with corrections as necessary. The LCAO method is considered in overview in Section 5.2. Before delving into LCAO, however, it may be helpful to review some of the results and to look at the bonding behaviors schematically.

In the discussion below we will need of the following terms:

Homopolar semiconductors: All atoms in the unit cell in these materials are the same so there is no charge transfer from one atom to another. Examples of such materials are Si and Ge. In these two examples, there are two atoms per primitive unit cell but both are the same kind of atom.

Heteropolar semiconductors: There are two or more different kinds of atoms organized regularly in the unit cell. These transfer electrons from one atom to the other and thus have different polarities. Examples of such materials are GaAs and AlN. In such materials the atoms are well organized into a compound (as distinct from a random alloy) with a specific lattice structure.

Note: A Si-Ge alloy has two kinds of atoms but they mix randomly and specific sites for one or the other cannot be distinguished. Therefore, such a mixture is an alloy of homopolar materials, not a heteropolar compound.

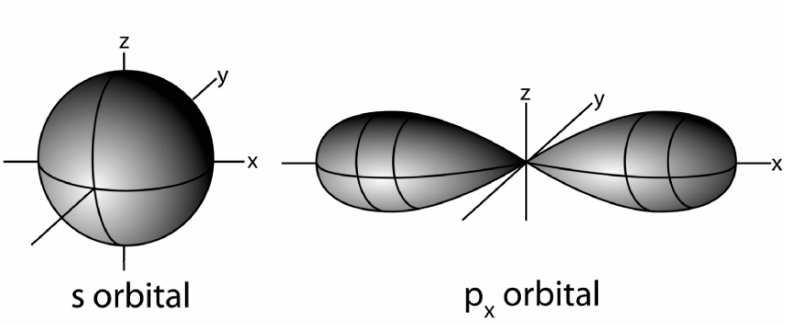

$$\psi_s = \frac{2a_0^{-3/2}}{\sqrt{\pi}}\left(1-\frac{r}{2a_0}\right)e^{-r/2a_0} \qquad \psi_{px} = \frac{2a_0^{-3/2}}{\sqrt{\pi/3}}\left(1-\frac{r}{2a_0}\right)e^{-r/2a_0}\cos\theta$$

Figure 5.1: Shows the shape of the s and p_x orbitals and the equations that describe them. a_0 is the atomic orbital size, r is the radius from the nucleus, and θ is the angle in the x,y plane.

5.1.1 Homopolar semiconductors

We begin the discussion by considering isolated atoms. Atoms have electron orbitals determined by solution of the Schrödinger equation for a positive core potential. The only case that can be solved explicitly is the hydrogen atom or a single electron orbiting a more highly charged nucleus. Atoms with multiple electrons are very hard to treat exactly, due to the difficulty in dealing with the correlations of motions of electrons with each other. Fairly good quantum chemical methods have been developed for approximating the correlated many-electron systems. While exact analytical solutions for the multi-electron case are not possible, the general phenomena found in single electron states holds true for multi-electron atoms, and correlation effects represent only perturbations on the single-electron behaviors.

Each atomic orbital is described by a series of quantum numbers (n, m, l, s), corresponding to the properties of total (n), orbital (m, with $0 \le m \le n$), and azimuthal (l, with $|l| \le m$) angular momenta, and spin ($s = \pm 1/2$). For m=0 the orbitals are spherical and are termed "s" orbtials. For m=1 the orbitals have roughly figure-eight shaped probability distributions along one of the three coordinate axes and are termed "p" orbitals, one for each value of l. The m=2 and m=3 values give the "d" and "f" orbitals. Spin allows two electrons per orbital for each of the various s, p, d, and f states. The geometries and basic mathematical descriptions of the s and p atomic orbitals are given in Figure 5.1. Their derivations for the hydrogen atom may be found in most undergraduate quantum mechanics textbooks. Each orbital has a well-defined [binding] energy, which increases with increasing nuclear charge. The

specific energies were observed over 120 years ago through their effect on the optical emissions of flames. The energies of all orbitals are commonly observable today by many techniques. Two of the more precise but accessible methods of direct observation of these states are x-ray photoelectron spectroscopy and Auger electron spectroscopy.

When two or more atoms bond together to form a molecule, the atomic orbitals may be considered to be mixed together to form molecular hybrid states. The hybrids are atom-like in that they are localized. However, they have the geometry of the molecule. Thus, they are generally termed molecular, rather than atomic, orbitals. For example, when a water molecule forms it has a bond angle between the two hydrogen atoms of 108°. This is because the three 2p orbitals and one 2s orbital of the oxygen have combined to form four $2sp^3$ hybrid orbitals pointing toward the vertices of a tetrahedron, and are therefore separated by 108°. Two of the orbitals are completely full of oxygen electrons while the other two have one opening each, which is filled by the hydrogen electrons. The shapes of sp^3 and similar sp^2 hybrid orbitals are shown in Figure 5.2. Both are common in semiconductor bonding. In the following discussion we will consider the consequences of sp^3 bonding on the energy of electrons in diamond or zincblende-structure semiconductors. A similar argument can be made for sp^2 bonding with respect to hexagonal wurtzite-structure materials. As we will see in Section 5.2, the hybrid orbital picture is equivalent to considering the interaction of each orbital with all others individually and adding the resulting interactions together. The advantage of the hybrid picture is that it shows why the resulting crystals have the symmetry and structure that they have.

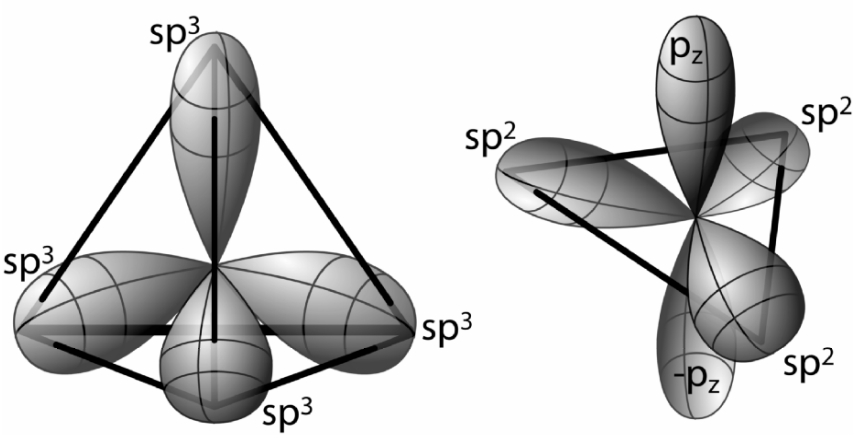

Figure 5.2: Shows the symmetry of the hybridized sp^3 and sp^2 molecular orbitals. The sp^2 orbitals lie in a plane perpendicular to the p_z orbitals and are equal lengths. The sp^3 orbitals are all equivalent to each other and stretch to corners of a tetrahedron.

Atoms from which diamond-structure and hcp semiconductors are constructed have three partially filled p valence-state (lowest binding energy) orbitals with energies close to the filled valence s-states. When the atoms come together to form the semiconductor, their one outer s state and three valence p states can be viewed as mixing to form sp^3 hybrid orbitals. This configuration maximizes the number of electron pairs, and makes each final bond as similar and as low energy as possible. The energy of the hybrid orbital is the linear average of the starting orbitals:

$$E_{sp^3} = \frac{1}{4}\left(E_s + 3E_p\right). \tag{5.1}$$

So far we have not changed the average energy of the orbitals, although the system began, for example in silicon, with two electrons in the 3s orbital and two in the three 3p orbitals. Therefore, the average energy of the electrons has increased as a result of the hybridization process, from the initial state $E_i=2E_s+2E_p$ to the final state $E_f = 4E_{sp3} = E_s+3E_p$. This would be energetically unfavorable if it were not for the formation of bonds between these orbitals. Hybridization is always energetically unfavorable for individual atoms, which is why the orbitals for isolated atoms are as they are and do not occur as hybrids. To see why hybridization does occur in solids, we construct wave functions that are linear combinations of two sp^3 orbitals:

$$\begin{aligned} \psi_u &= \psi_1^{sp^3} - \psi_2^{sp^3} \\ \psi_g &= \psi_1^{sp^3} + \psi_2^{sp^3}, \end{aligned} \tag{5.2}$$

where ψ_g is the symmetric combination of the hybrid sp^3 wave functions of the individual atoms and ψ_u is the antisymmetric combination. (The g and u subscripts refer to the German words for symmetric and antisymmetric, gerade and ungerade. Some authors reverse the g and u labeling scheme.) These combinations are similar to those that appear in Chapter 2 for the nearly free electron model (Equation 2.5) and which gave rise to the higher or lower energy bands at the zone boundary (Equation 2.10). The symmetric combination lowers the energy of the electrons as the atoms approach each other and is referred to as a "bonding" orbital. The anti-symmetric combination raises the energy with respect to the starting states and is termed an "antibonding" orbital. When ψ_1 and ψ_2 are half-filled, the combination of the two contains enough electrons to exactly fill the bonding orbitals and leave the antibonding orbitals empty. The situation is shown schematically in Figures 5.3 and 5.4. Note that in this case we have gained as much energy from the bonding process as possible by placing all electrons in the lower energy states and no electrons in the higher energy states. This is why semiconductors have such strong bonds.

The nature of bonding can be seen immediately from a consideration of the effect on electron density of symmetric and antisymmetric linear combinations of the wave functions ψ_1 and ψ_2. Consider for simplicity the interaction of two s-orbitals. (The sp^3 hybrids behave essentially the same way but with more complex geometry.)

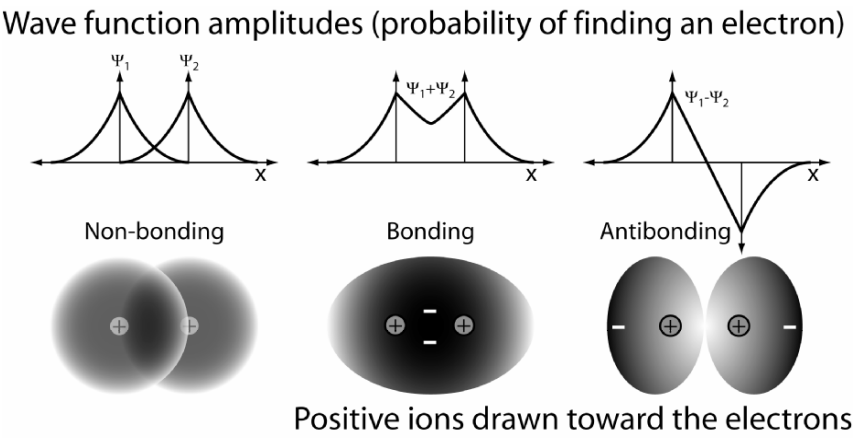

Figure 5.3: A schematic diagram illustrating the basis of cohesion in solids resulting from symmetric and antisymmetric combinations of atomic orbitals. The center of electron charge lies between the positive ions for a symmetric bonding orbital and outside of the positive ions for an antisymmetric orbital combination.

S-like atomic wave functions are peaked around the positively-charged nucleus of an atom and decay with distance from that atom (see Figures 5.1 and 5.3). A symmetric sum of the two, ψ_g, has a high intensity between the two atomic nuclei, twice the magnitude of a single wave function at half the interatomic distance. By contrast, the antisymmetric wave function, ψ_u, has a node (ψ_u=0) at the midpoint between the atoms. In the symmetric case there is a high density of negative charge between the atoms, which attracts the positive nuclei and holds the atoms together. This is the source of cohesion in the bonded pair. In the antisymmetric case, the wave function amplitude is depressed between the atoms and the positively-charged nuclei are relatively exposed to each other. This leads to repulsion. When only the symmetric state is filled with electrons, the maximum bonding occurs. When both states are completely filled the attractive and repulsive forces match and result in no net bonding.

The energy difference between the bonding or antibonding states and the hybrid molecular orbital energy is referred to as the homopolar energy, V_2 and the bonding-antibonding orbital energy difference is $2V_2$. V_2 can be shown [see Harrison, Ref. 1 for example] to depend approximately upon the inverse square of the interatomic distance, d, as:

$$V_2 \approx 4.4\frac{\hbar^2}{md^2}\,\text{eV}. \qquad 5.3$$

Thus, as the atoms approach each other, the bonding strength increases rapidly (as $1/d^2$) until the repulsion of the positively-charged atomic cores begins to become significant. So far, however, we only have two atoms bonded into a dimer molecule. As more and more atoms are added, all of the atomic or molecular states of all of the atoms interact with each other. These interactions are between second, third, and increasingly higher-order neighbors and are progressively weaker as the solid becomes larger. It is these interactions which lead to the continuum of states we call a band. Their collective interaction is best described with waves as in Chapter 2.

A more complete analysis shows that the bands broaden following the same $1/d^2$ functionality as for the homopolar splitting V_2. However, because the broadening of the bands is relatively weak overall compared to the increase in their separation, the direct energy gap still increases with decreasing interatomic distance. In other words, the factor scaling $1/d^2$ in the band broadening term is smaller than the constant in Equation 5.3. The dependence of V_2 and energy gap on d is ultimately responsible for the pressure and temperature dependences of the energy gap in homopolar semiconductors (see Section 5.4).

The cohesive energy of the homopolar solid is just the amount by which the average electron's energy is reduced in going from the original atomic orbitals through the hybridization process to the formation of bonding and antibonding states and finally to the formation of bands. The greater the energy difference between the bonding and antibonding states ($2V_2$), the higher the cohesive energy of the material. For the simple bonding-antibonding states (not the bands) of Figure 5.4, the cohesive energy would be the average energy (increase) of an sp^3 hybrid state relative to the starting s and p states, $[(E_s+3E_p)-(2E_s+2E_p)]/4 = (E_p-E_s)/4$ per electron, less the energy gained by bonding, V_2 for each of the eight electrons in the unit cells (4 electrons per atom with a two atom basis in the diamond structure). Thus,

$$E_{cohesive} = 2\left(E_p - E_S\right) - 8V_2. \qquad 5.4$$

The true cohesive energy is this value modified by the average change in energy for electrons during formation of bands from individual bonded molecular orbitals. This difference corresponds to the average energy of the valence band relative to the bonding state. One can guess that this will be favorable for any material in which formation of the complete solid (consequently formation of bands) occurs. It could be unfavorable for cases such as diatomic gases although at low enough temperatures these materials do solidify. However, in all normal semiconductors the formation of bands is quite favorable and the average energy of the band is below that of the molecular orbital.

5.1.2 Heteropolar compounds

The picture in the previous section works well when there is only one type of atom in the material. When there are chemically different atoms, their electron densities, electron affinities, and nuclear charges differ. Because of this, their atomic orbitals

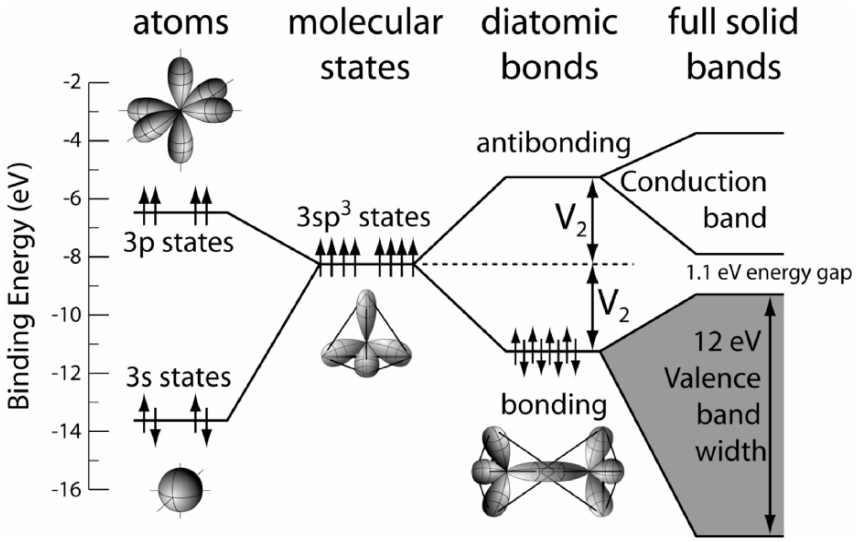

Figure 5.4: A schematic diagram of the evolution of bonding of Si atoms. The filled 3s and partially filled 3p atomic orbitals of two atoms combine to form half-filled sp^3 hybrid molecular orbitals. These combine to form bonding and antibonding orbtials. As more atoms collect atoms collect to create a bulk solid, bands form.

have different energies. The easiest way to see this is to compare two atoms in the same row. For example, compare Ga with As. Both have filled 1s, 2s, 2p, 3s, 3p, and 4d core states and filled 4s valence states. In addition, each has a partially filled set of 4p valence orbitals. Ga has only one electron in its 4p orbitals, while As has three. The energy binding the 4p electrons is the same within a given atom, but the two additional positive charges in the nucleus of the As atom hold the three 4p electrons much more strongly than the weaker nuclear charge of the Ga nucleus holds its single 4p electron. This means that the 4p state in As is much lower in energy (stronger electron binding) than the 4p state in Ga. Likewise, the 4s orbital energies are affected by the additional nuclear charge. Consequently, the hybrid sp^3 orbitals of the two atoms come out at much different energies. This energy difference is shown schematically in Figure 5.5 and is twice the quantity termed the chemical splitting, C. Mathematically,

$$2C = E_c^{sp^3} - E_a^{sp^3} \qquad 5.5$$

at some ideal interatomic distance, where E_c and E_a refer to the energies of the cation and anion molecular orbitals, respectively. The values of chemical splitting increase as the atoms move farther apart on the periodic table in a given row (larger difference in electronegativity). As the interatomic distance shrinks the chemical splittings increase, as discussed below.

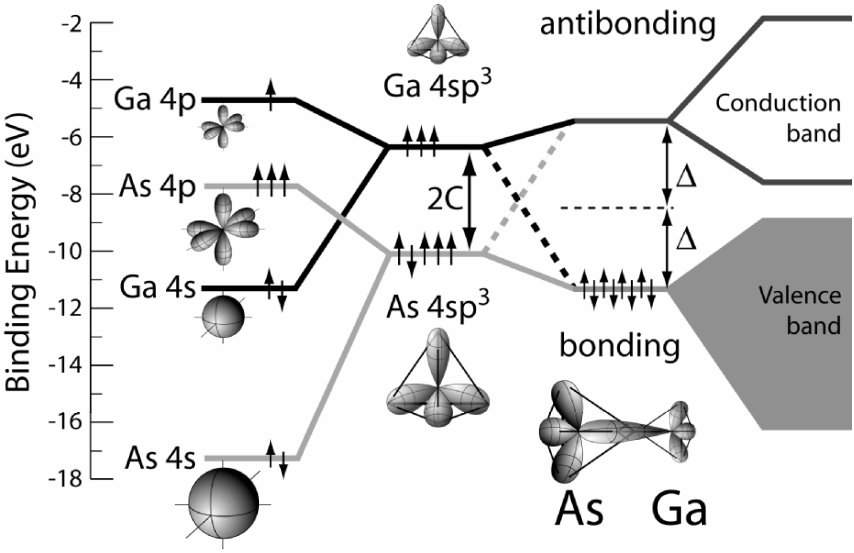

Figure 5.5: Shows the evolution of atomic orbital energies to form bonds and ultimately bands. The geometries of the atomic and hybrid orbitals are shown schematically as insets.

Heteropolar semiconductors can be thought to form sp^3 hybrid molecular orbitals exactly as do homopolar semiconductors. When we considered two atoms together in a homopolar semiconductor, bonding and antibonding states resulted from symmetric and antisymmetric mixtures of identical hybrid orbitals. The same combinations occur in a heteropolar semiconductor, but now the cation and anion hybrid orbitals sp^3_C and sp^3_A are more distinguishable and have different electron densities. Furthermore, the symmetric and antisymmetric states now have different contributions from the cation and anion molecular orbitals.

Thus, Equation 5.2 becomes:

$$\begin{aligned}\psi_u &= u_2\psi_a^{sp^3} - u_1\psi_c^{sp^3} \\ \psi_g &= u_1\psi_a^{sp^3} + u_2\psi_c^{sp^3},\end{aligned} \qquad 5.6$$

where u_1 and u_2 are coefficients which describe the relative contribution of the anion and cation to the antibonding and bonding states. Both are related to the square root of the bond polarity, as discussed below. Furthermore $u_1^2+u_2^2=1$. The separation of these states is now a combination of a homopolar splitting, V_2, type term and a

chemical splitting, C term. The resulting separation, Δ, (see Figure 5.5) is given approximately (see Harrison, Ref 1, for discussion and derivation) as:

$$\Delta = \sqrt{C^2 + V_2{}^2}\,. \qquad 5.7$$

The homopolar splitting component, V_2, of a heteropolar bond increases exactly as for a homopolar semiconductor according to Equation 5.3 as the interatomic spacing decreases. The chemical splitting also increases with decreasing bond distance d, approximately (see Ferry for discussion) as:

$$C = c\left(\frac{Z_A}{r_A} - \frac{Z_C}{r_C}\right)e^{-k_{TF}d} \qquad 5.8$$

where Z_A and Z_C are the anion and cation atomic numbers, r_A and r_C are their covalent radii, $d=r_A+r_C$ is the interatomic distance, k_{TF} is the Thomas-Fermi screening length (the distance over which electrons in a solid screen an extenally-applied electric field), and c is a constant. For typical semiconductors, k_{TF} is in the range of 0.1 nm. One should be cautious in applying the formulas 5.5 through 5.8 too closely as detailed band structure calculations yield somewhat different values (see discussion in Section 5.2) than one would infer from the simple formulas. However, these formulas provide illustrative examples of the general functional form of the variables.

Because C and V_2 increase rapidly with decreasing interatomic distance, the bonding and antibonding states move away from each other as interatomic distance decreases. This has important consequences. For example, as with the homopolar materials, this effect is directly responsible for the temperature and pressure dependence of the direct energy gap (see Section 5.4). Because the chemical splitting increases roughly exponentially with decreasing distance, while homopolar splitting increases only quadratically, the chemical splitting becomes increasingly dominant at small interatomic distances. This also leads to more polar bonding as bond length shrinks, as we will see below.

It is now time to return to the observation that the cation and anion molecular sp^3 orbitals do not contribute equally to the symmetric and antisymmetric molecular orbitals (Equation 5.6), i.e. $u_1 \neq u_2$. Because of the way in which orbitals combine, the molecular orbital that is closest in energy to the bonding or antibonding state contributes most to that state. Thus, the lower binding energy state associated with the cation contributes most to the antibonding orbitals. Likewise, the higher binding energy anion contributes most to the bonding state. This is indicated schematically in Figure 5.5 by the solid and dashed lines connecting the bonding and antibonding states to the cation and anion molecular orbitals. Solid lines show the primary contribution while dashed lines indicate a minority contribution. The mixing of the states will be discussed in more detail in Section 5.2, which provides a more specific justification for this difference.

If the antibonding states are empty and the bonding states are filled, the localization of the states results in a difference in the charge density around the cation and anion. In other words, as the bands become increasingly connected to given atoms, the bonding becomes more ionic. A quantitative relationship between chemical splitting and ionic character, α, of the bonds can be derived (see, for example Harrison) to be:

$$\alpha = \frac{C}{\Delta} = \sqrt{\frac{C^2}{V_2^{\,2} + C^2}}\,. \qquad 5.9$$

The increase in ionic bonding also applies as the atoms are forced closer together. Likewise ionic character will change with pressure and temperature. One can go further and determine that $u_1=[(1+\alpha)/2]^{1/2}$ and $u_2=[(1-\alpha)/2]^{1/2}$ (see Harrison, for example). One can then calculate u_1 and u_2 terms of C and V_2 using Equation 5.9.

$$u_1^2 = \frac{1+\sqrt{C^2/\left(V_2^2+C^2\right)}}{2} \text{ and } u_2^2 = \frac{1-\sqrt{C^2/\left(V_2^2+C^2\right)}}{2} \qquad 5.10$$

For the case of a completely ionic bond, α=1, and the bonding and antibonding states are entirely composed of anion and cation states, respectively.

It may be helpful for the reader to consider some specific numerical values for some of these constants for common semiconductors. Atomic orbital energies for selected elements are given in Table 5.1. A full table of values may be found in Harrison. Table 5.2 gives data for homopolar and chemical splittings as well as minimum energy gaps for several semiconductors based on values from Ferry. The reader will find that the constants C and V_2 calculated using information in Table 5.1 based on the formulae above do not result in the numbers in Table 5.2. This is because of the various corrections to the results, which are necessary in an accurate calculation of a band structure and not included in the simplified approach resulting in the above. Some of these corrections have been included in the values in Table 5.2. Full band structures for several compounds are described in Section 5.3, and many more may be found in the literature. Once again, although *the formulas in this section are not sufficient to predict accurate band behaviors*, they do provide useful trends and explain the basis of many experimental results.

The observations about atomic contributions to bonding and antibonding states become more relevant when we realize that these states make up the valence and conduction bands. Therefore, a change in the cation, keeping the anion the same, will primarily affect the conduction band, while a change in the anion for a constant cation primarily affects the valence band. This leads to the common cation and common anion rules as well as to the relative magnitudes of the band offsets, which we encountered in Chapter 3. The ratio of the energy band offsets, $\Delta E_V/\Delta E_C$ directly reflects the relative magnitudes of the coefficients u_1 and u_2 in Equation 5.10 across a heterojunction.

Table 5.1: **Atomic and Molecular Orbital Energies**

Atom	E_s (eV)	E_p (eV)	E_{sp3} (eV)	Atom	E_s (eV)	E_p (eV)	E_{sp3} (eV)
C	17.52	8.97	11.11	**Ge**	14.38	6.36	8.37
Si	13.55	6.52	8.28	**Sn**	12.50	5.94	7.58
Al	10.11	4.86	6.17	**P**	17.10	8.33	10.52
Ga	11.37	4.90	6.52	**As**	17.33	7.91	10.27
In	10.12	4.69	6.05	**Sb**	14.80	7.24	9.13
Mg	6.86	2.99	3.96	**S**	20.80	10.27	12.90
Zn	8.40	3.38	4.64	**Se**	20.32	9.53	12.23
Cd	7.70	3.38	4.46	**Te**	17.11	8.59	10.72
Cu	6.92	1.83	3.10	**Br**	23.35	11.20	14.24
Ag	6.41	2.05	3.14	**I**	19.42	9.97	12.33
Values from Walter A. Harrison, Ref. 1.							

Table 5.2: **Bond Orbital Energies**

Molecule	**Interatomic Distance (Å)**	**Homopolar Splitting $2V_2$ (eV)**	**Chemical Splitting, 2C (eV)**	**Bond Energy, 2Δ (eV)**	**Minimum 300 K Energy Gap (eV)**
C	1.54	13.88		13.88	5.4
Si	2.35	5.96		5.96	1.107
AlP	2.36	5.92	3.48	6.87	2.5
Ge	2.44	5.52		5.52	0.67
GaAs	2.45	5.48	3.02	6.26	1.42
ZnSe	2.45	5.55	3.80	6.73	2.58
CuBr	2.49	5.37	5.59	7.75	2.94
Sn	2.80	4.20		4.20	0.08
InSb	2.81	4.16	2.56	4.88	0.165
CdTe	2.81	4.16	5.22	6.67	1.44
Values from D.K. Ferry, Ref. 2. Minimum energy gaps from Ref. 3.					

5.2 LCAO: FROM ATOMIC ORBITALS TO BANDS

Although the hybrid molecular orbital description of how bonds form is most convenient for a simple picture of the geometry of specific compounds, a more precise and general result can be obtained by keeping the original atomic orbitals in the scheme. This section considers how this may be accomplished and delves deeper into the methods for calculating of real E(k) diagrams. Even so, many details are glossed over. For a complete description of the methods the reader is referred to the suggested readings. For this discussion we will follow the linear combination of atomic orbitals (LCAO) approach. Note that in spite of the difference between

considering atomic orbitals individually and using the hybrid orbitals, the results are identical as long as only the states that enter into the hybrid contribute to bonding.

The beginning of the LCAO approach is the valence atomic orbitals of the atoms forming bonds. In most semiconductors the important states are the s and p orbitals. In some cases other orbitals such as shallow-lying (outermost) d-states contribute significantly to the complete picture of bonding. For now we will ignore such complications. This is safe for the case of Si where no d-state electrons are present but not, for example, for GaAs. An analysis of orbital interactions requires selection of a coordinate system. It is conventional, for example, to orient the p-orbitals along the Cartesian coordinate axes. From this point it is easy to construct the sp^3 hybrid orbitals along bond directions in a diamond-structure material:

$$\begin{aligned}
\psi_{[111]} &= (\psi_s + \psi_{p_x} + \psi_{p_y} + \psi_{p_z})/2 \\
\psi_{[\bar{1}\bar{1}1]} &= (\psi_s - \psi_{p_x} - \psi_{p_y} + \psi_{p_z})/2 \\
\psi_{[\bar{1}1\bar{1}]} &= (\psi_s - \psi_{p_x} + \psi_{p_y} - \psi_{p_z})/2 \\
\psi_{[1\bar{1}\bar{1}]} &= (\psi_s + \psi_{p_x} - \psi_{p_y} - \psi_{p_z})/2
\end{aligned} \qquad 5.11$$

Here the crystallographic indices in the subscripts refer to the hybrid molecular orbital directions. Because the Schrödinger Equation governing electron motion is linear, any combination of wave functions that solve it will also be a solution. In other words, choosing the hybrid orbitals or the atomic orbitals as a starting point for the calculation must yield identical results. The most flexible and general approach is not to be restricted to specific hybrid orbitals but rather to consider all possible orbital-by-orbital interactions of the fundamental atomic states. These states apply to a given atom in any environment. Thus, their use is valid for any material in which the atom occurs. As an example of a specific interaction, one can ask how does the p_x orbital on one atom interact with the p_z orbital on another atom.

To answer this, some additional terminology will be useful. Electron states having at least some component of their orbitals parallel to one another can interact in two ways. When the bonds (or projected components of the bonds) are parallel to the orbital axis, this results in a "σ" bond, while bonds perpendicular to the orbital axes are "π" bonds. Thus, s-orbitals always form σ bonds (they have no specific axis) while p-orbitals can have σ -like and π -like characters. When interacting orbitals do not lie directly along or orthogonal to a bond axis, one can decompose the resulting interactions into σ-like and π-like portions as well as a portion for which the orbitals are orthogonal to one another and therefore have no interaction. This leads to a series of geometric coefficients, which scale the interactions for each pair of states according to their orbital axes, relative positions, and symmetries. Sketches of the s and p orbitals in a diamond-lattice semiconductor along with some of their interactions are shown in Figure 5.6. Note how none of the p-orbitals point directly along bond directions for the conventional choice of axes. However, the orbitals can

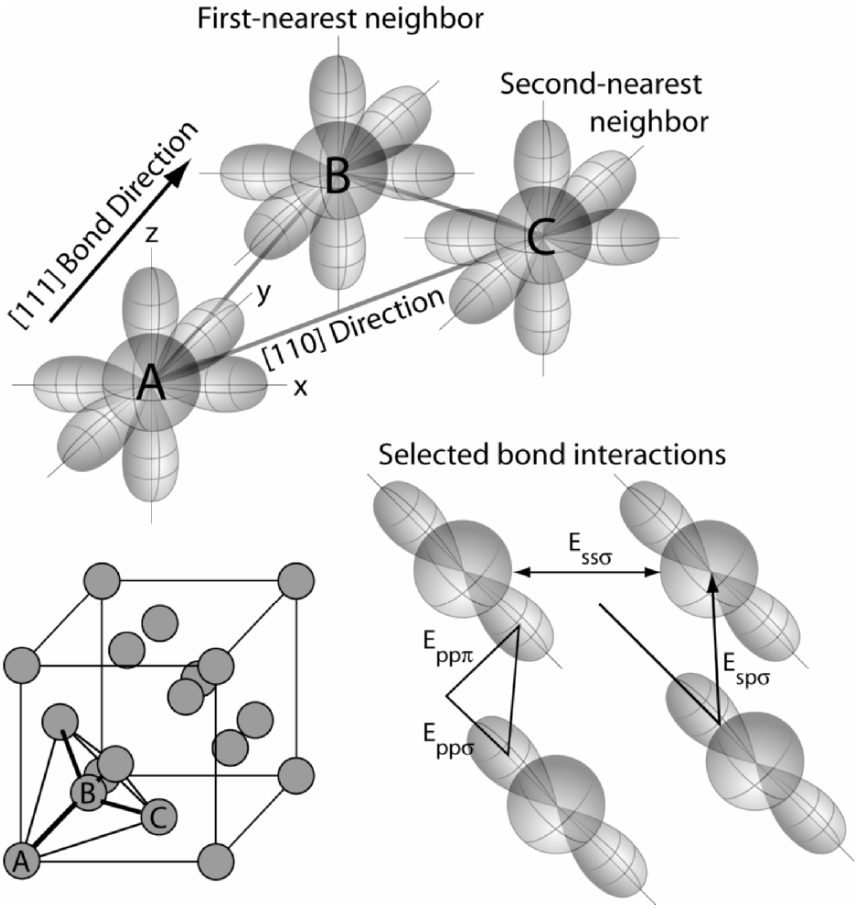

Figure 5.6: A schematic diagram showing the interactions of selected atomic orbitals and the geometry of these orbitals with respect to the crystal lattice in a zincblende or diamond structure material.

be decomposed into a component directed toward another orbital, a component parallel to another orbital (π-like bond), and a perpendicular component. If the axes were chosen such that a given pair of orbitals lay directly along that axis, the others would have reduced components along those directions and the result would be the same. Choice of coordinate axes is irrelevant to the result.

The coefficients of each interaction represent the relative strength and component of the interaction for a given bond. For the situation shown in Figure 5.6, the energies of the possible interactions may be shown to be [1]:

$$\begin{aligned} E_{ss} &= V_{ss\sigma} \\ E_{sp} &= -\frac{V_{sp\sigma}}{\sqrt{3}} \\ E_{xx} &= \frac{V_{pp\sigma}}{3} + \frac{2V_{pp\pi}}{3} \\ E_{xy} &= \frac{V_{pp\sigma}}{3} - \frac{V_{pp\pi}}{3} \end{aligned}, \qquad 5.12$$

where $V_{ss\sigma}$, $V_{sp\sigma}$, $V_{pp\sigma}$, and $V_{pp\pi}$ describe the strengths of the ss σ-bonds, the sp σ-bonds, the pp σ-bonds, and the pp π-bonds, respectively, for a given interatomic distance and type of atom. The interaction potentials, V, are then scaled by the projections of the p orbitals along the x,y, and z axes in the directions of the orbital with which they are interacting, leading to the final interaction energies of Equation 5.12. E_{xx} refers to the interaction of a p-orbital with another p-orbital on an adjacent atom along the same axis; for example, a p_x orbital interaction with another p_x. E_{xy} refers to the interaction of a p-orbital pointed along one axis with a p-orbital on an adjacent atom pointed along one of the other two orthogonal axes. (Although the axes are orthogonal, the orbitals are not, see Figure 5.6.) To repeat for emphasis: the V's are orientation and axis-independent interaction potentials while the E's are these interaction terms projected along specific axes. Harrison gives approximate formulas for atom-independent values of V from which values for the various E's can be estimated for a given lattice. According to Harrison, all V's, and hence all E's, scale as $\hbar^2/md^2$, from which Equation 5.3 results [$\hbar^2/\boldsymbol{m}$ = 0.0762 eV-nm^2]. In units of $\hbar^2/md^2$, the resulting values of the E's would be: E_{ss}=-1.4, E_{sp}= -1.06, E_{xx}=0.54, and E_{xy}=1.35 based on Equation 5.12. These coefficients, along with phase factors describing the phase of the Bloch waves in the solid figure into a matrix describing all of the possible pairwise bond interactions.

It is through the phase factors that a given electron momentum is defined. One might have expected this as, from the discussion of Chapter 2, band structures represent the interference of electron waves with the periodic potential of the lattice. For the wave functions in Equation 5.10, the corresponding phase factors are:

$$\begin{aligned} g_0(k) &= e^{ik\bullet d_{111}} + e^{ik\bullet d_{\bar{1}\bar{1}1}} + e^{ik\bullet d_{1\bar{1}\bar{1}}} + e^{ik\bullet d_{\bar{1}1\bar{1}}} \\ g_1(k) &= e^{ik\bullet d_{111}} - e^{ik\bullet d_{\bar{1}\bar{1}1}} + e^{ik\bullet d_{1\bar{1}\bar{1}}} - e^{ik\bullet d_{\bar{1}1\bar{1}}} \\ g_2(k) &= e^{ik\bullet d_{111}} - e^{ik\bullet d_{\bar{1}\bar{1}1}} - e^{ik\bullet d_{1\bar{1}\bar{1}}} + e^{ik\bullet d_{\bar{1}1\bar{1}}} \\ g_3(k) &= e^{ik\bullet d_{111}} + e^{ik\bullet d_{\bar{1}\bar{1}1}} - e^{ik\bullet d_{1\bar{1}\bar{1}}} - e^{ik\bullet d_{\bar{1}1\bar{1}}} \end{aligned}. \qquad 5.13$$

An examination of the terms for the g values will show that these simply represent the interference behavior of the electron waves with given wave vectors **k** interacting with atoms at positions defined by the real-space vectors **d** and at the origin. The g values include the free-electron-like behavior of Chapter 2. The calculation of the g factors becomes more complex when second-nearest neighbors and beyond are included, but the method is the same. The energy of an electron with wave vector **k** is the determinant of a matrix representing the energies of all possible orbital pairs. For example, for a zincblende semiconductor with no d-orbitals the LCAO matrix is [c.f. Ref. 4]:

	s_c	s_a	p_{xc}	p_{yc}	p_{zc}	p_{xa}	p_{ya}	p_{za}
s_c	E_{sc}	$E_{ss}g_0$	0	0	0	$E_{sp}g_1$	$E_{sp}g_2$	$E_{sp}g_3$
s_a	$E_{ss}g_0^*$	E_{sa}	$-E_{sp}g_1^*$	$-E_{sp}g_2^*$	$-E_{sp}g_3^*$	0	0	0
p_{xc}	0	$-E_{sp}g_1$	E_{pc}	0	0	$E_{xx}g_0$	$E_{xy}g_3$	$E_{xy}g_2$
p_{yc}	0	$-E_{sp}g_2$	0	E_{pc}	0	$E_{xy}g_3$	$E_{xx}g_0$	$E_{xy}g_1$
p_{zc}	0	$-E_{sp}g_3$	0	0	E_{pc}	$E_{xy}g_2$	$E_{xy}g_1$	$E_{xx}g_0$
p_{xa}	$E_{sp}g_1^*$	0	$E_{xx}g_0^*$	$E_{xy}g_3^*$	$E_{xy}g_2^*$	E_{pa}	0	0
p_{ya}	$E_{sp}g_2^*$	0	$E_{xy}g_3^*$	$E_{xx}g_0^*$	$E_{xy}g_1^*$	0	E_{pa}	0
p_{za}	$E_{sp}g_3^*$	0	$E_{xy}g_2^*$	$E_{xy}g_1^*$	$E_{xx}g_0^*$	0	0	E_{pa}

5.14

Subscript "a" designates atomic orbitals due to the anion while subscript "c" designates the cation orbitals. The energies on the diagonal of the matrix are the energies of the atomic orbitals for cations or anions. Values for such energies were given for selected elements in Table 5.1. The g values are complex numbers. To obtain proper behavior from the matrix, complex conjugates of g must be included such that elements across the diagonal are conjugates of one another. These conjugate values are indicated by an "*". The negative terms result because in some cases the negative lobe of the wave function is interacting with a positive lobe of another. Thus, the negative coefficient gives an attractive interaction.

Additional rows and columns should be added to the matrix for more complex compounds with more than two atoms and the formula for the g's becomes much more complex. The matrix also expands when shallow-lying d-orbitals must be taken into account. Simpler structures such as the diamond lattice have a smaller interaction matrix because there is no distinction between cation and anion sites. The matrix may also be modified by effects such as spin-orbit splitting. (Spin-orbit splitting is one of the corrections necessary to an accurate band calculation. It results from the interaction of the electron spin magnetic moment with the dot product of its velocity and the local electric field due to the positive atomic cores of the lattice.) Likewise, greater accuracy can be obtained if additional terms are included in the g values to account for second and higher neighbors.

One may wonder how to interpret this matrix in light of the nearly free electron model of Chapter 2 and the discussions at the beginning of this chapter. The Schrödinger equation enters into the matrix through the calculations of the individual interaction energies of various electron orbitals with one another; in other words, the $V_{ss\sigma}$, $V_{sp\sigma}$, $V_{pp\sigma}$, and $V_{pp\pi}$ terms that appear in Equation 5.12. These terms and the cation and anion orbital energies are also the only places that chemical differences appear in the problem. From the V values, the interaction energies for a given geometry of the lattice may be determined by projection of the orbitals onto the bond directions (Equation 5.13). As noted above, the matrix simply represents the set of equations for the linear combination of all atomic orbitals in pairs. Each possible pair corresponds to a specific element of the matrix. We encountered one such linear combination in the nearly free electron model in Equation 2.9, but for the combination of only two wave functions. This then led to the energies in Equation 2.10. Another example of a linear combination of two electron waves is shown in Figure 5.3. The individual elements of the matrix give the strength and phase of the individual interactions. Note that some of the matrix elements in Equation 5.14 are zero where the orbitals are orthogonal to one another. (For example, on the same atom orbitals must be orthogonal and cannot interact.)

The eigenvalues of Equation 5.14 describe the complete band structure for the solid when one considers all possible real-space translation vectors **d** of the lattice and all reciprocal lattice electron wave vectors **k**. In principle, calculating the band structure of a real solid, such as those shown in the next section, should be no harder than making the appropriate substitutions for **d** and **k** in Equation 5.13, calculating the phase factors (g's), substituting these into Equation 5.14, and calculating the eigenvalues. However, if one uses "standard" orbital energies (Table 5.1), estimates the interaction potentials V from simple approximate (but easy to solve) versions of the Schrödinger equation, and if one substitutes these into Equations 5.12-5.14 and calculates a band structure, one will not immediately arrive at the true structure. A high quality band calculation requires inclusion of numerous corrections to the potentials determining the V values, spin-orbit effects, higher neighbor interactions in the g values, and shallow-lying d-bands, when present, etc. Discussions of the details of these corrections may be found in the suggested readings.

Such detailed calculations are integrated into many computational models, so fortunately it is not necessary for the average semiconductor engineer to know how to perform the analysis. However, in spite of the convenience of computational methods, it is important to use them with caution. Even the most sophisticated methods generally perform much better for specific portions of the energy band structure and are relatively unreliable for other portions, especially in an *ab-initio* application (where one is not fitting experimental data). Much more reliable results are obtained by fitting experimental values to correct the calculation, making the band structure models interpretive rather than predictive. The most extreme version of the fitting approach is the empirical tight-binding method where one simply adjusts all of the matrix elements (with best guesses as to relative ratios) in order to

match experimental data. One can then use the fit matrix elements to estimate energies of specific conformations of atoms via the g factors. The tight binding method makes little effort to actually determine the correct values of V from first-principles. In spite of the various concerns and caveats in the above discussion, band structure calculations are very useful in understanding trends in semiconductor behaviors and predicting optimal structures. Calculations are good for guessing the properties of a hypothetical semiconductor and therefore to semiconductor design.

We will consider some of the implications of the LCAO method next based on the above equations and ignoring detailed corrections. The simplest trend to understand is the behavior at Γ, where **k**=0. In this case Equation 5.13 yields g_0=4 and g_1, g_2, and g_3=0. This makes the interaction matrix exceedingly simple and results in the following four energies [1]:

$$E(\Gamma_{ss}) = \frac{E_{cs} + E_{as}}{2} \pm \sqrt{\left(\frac{E_{cs} - E_{as}}{2}\right)^2 + (4E_{ss})^2}$$
$$E(\Gamma_{pp}) = \frac{E_{cp} + E_{ap}}{2} \pm \sqrt{\left(\frac{E_{cp} - E_{ap}}{2}\right)^2 + (4E_{xx})^2}. \qquad 5.15$$

The $E(\Gamma_{ss})$ energy is for s-s bonds while the $E(\Gamma_{pp})$ energy results from the p-p bonds. Because at the Γ point $g_1 = g_2 = g_3 = 0$, there is no s-p bonding contribution. The "+" signs in Equation 5.15 represent antisymmetric antibonding states while the "-" signs correspond to the symmetric bonding states. Because the s orbitals have greater binding energies, the s-like states lie below the p-like states. Therefore, the top of the valence band and the top of the conduction band at Γ are composed of p-like states and the bottom of the valence and conduction bands are made up of s-like states. This means that **the band edges defining the energy gap of a direct-gap semiconductor of this type are p-like for the valence band and s-like for the conduction band.**

There are three p-p bonds with the same energy at Γ, one for each p-orbital axis. Thus, each of the two $E(\Gamma_{pp})$ energies refers to the energy of three separate branches of the E(k) diagram while only one branch occurs at each $E(\Gamma_{ss})$ energy. A more detailed analysis, including electron "spin-orbit" interactions in the calculation, [4] lowers the energy of one of the p bands. In addition, the curvatures of the two remaining bands are different and differ also from the split-off band. This leads to separate "light" (lower effective mass) and "heavy" hole behaviors. The two hole masses may be observed in some experiments sensitive to energetic holes.

Similar expressions to Equation 5.15 can be written for other parts of the band diagram. Relatively simple forms of the eigenvalues can be derived for the X and L

points, [1] which describe, in part, the behavior of the bottom of the conduction bands in Si and Ge. The X point is primarily dominated by s-p and p-p bonding interactions while the L point behavior is the same as at the Γ point but with ($2E_{xx}$+$2E_{xy}$) replacing $4E_{xx}$ in the expression for the p-p energy in Equation 5.15. One can see from these results that to obtain an indirect-gap semiconductor it is necessary to have relatively large values of E_{xy} and relatively small values of bond length.

The formulas for the various symmetry points such as Equation 5.15 give a strong indication of the trends in the bands and their relationships to the fundamental chemistry of the material. The results are the basis of the formulas in Section 5.1. As an example of how such relationships can be derived, let us try to explain why the minimum energy gap in a semiconductor might increase with decreasing lattice constant even though the homopolar splitting and the bandwidth increase together and might be expected to cancel out the bond-length effect. For simplicity, consider a homopolar semiconductor. In this case E_{cs}=E_{as}=E_s and E_{cp}=E_{ap}=E_p. Equation 5.15, then simplifies greatly and the band edges at the Γ point can be estimated (taking the appropriate signs) as:

$$\begin{aligned} E_c &= E_s + 4E_{ss} \\ E_v &= E_p - 4E_{xx} \end{aligned} . \qquad 5.16$$

The direct energy gap in a homopolar semiconductor is then E_{gap}=E_c-E_v, or

$$E_{gap}(\Gamma) = E_s - E_p + 4(E_{ss} + E_{xx}). \qquad 5.17$$

Substituting from Equation 5.12, one may then obtain

$$E_{gap}(\Gamma) = E_s - E_p + 4[V_{ss\sigma} + (V_{pp\sigma} + 2V_{pp\pi})/3]. \qquad 5.18$$

E_s and E_p are atomic orbital energies and are independent of bond formation and hence of bond length. If one examines Equation 5.18 one finds that the term in brackets resembles in some respects what one would get for a triple bond between two semiconductor atoms – contributions from one s-s σ-bond, one p-p σ-bond, and two p-p π-bonds. We can now answer the question at hand – how does $E_{gap}(\Gamma)$ change as the bond length changes. By examination of the values in Table 5.1, one finds that there is no consistent trend in E_s-E_p for the homopolar semiconductors. However, all of the wave function overlap energies V increase with decreasing interatomic distance. This shows why the net energy gap increases with decreasing atomic separation. A similar result is obtained in the heteropolar case. Therefore, we would expect a net change in energy gap, even though one might expect bandwidth and band-to-band spacing to offset one another.

One might also ask why it is necessary for an ordinary semiconductor engineer to worry about these details unless they were planning to pursue a graduate degree in semiconductor physics. The reason is that many aspects of semiconductor alloy and defect behaviors can be traced back to the phenomena discussed above. Furthermore,

there are many exceptions to the simple rules of thumb. Even the common cation and common anion rules can appear to be violated in complex materials. Therefore, a more detailed understanding of the sources of bonding is necessary to have a good sense of how to engineer band structures and defects. To illustrate the value of the LCAO approach to understanding semiconductor behavior, consider the following case.

The individual bond-by-bond interactions contribute to different parts of the bands in materials. This may mean that while the valence band may be expected to result primarily from anion atomic orbitals, the states near the valence band edge may be dominated instead by particular atomic states from a cation. Such complications do not arise significantly in simple semiconductors with strongly covalent and strongly sp^3-like bonds, as in GaAs. However, in a complex ternary compound semiconductor such as $CuInSe_2$ this type of behavior has an important effect. In the case of this compound, the bottom of the conduction band is primarily derived from In atomic states, as one would expect based on the behavior illustrated in Figure 5.5 and represented by Equations 5.5-5.9. At the same time, the top of the valence band is primarily due to Cu-Se bonds. Therefore, replacing Se with S will primarily affect the valence band edge even though the cations are in common. Replacing In with Ga strongly modifies the conduction band edge and will have almost no effect on the valence band. This behavior illustrates the subtlety of bonding in complex compound semiconductors (and similarly complex insulators and metals) and shows how exceptions to common cation and common anion rules may occur or where alloying may have a surprisingly large effect on one or the other band edge. Likewise, breaking the symmetry of the system by strain may affect different parts of the energy gap differently (see band offset discussion for Si-Ge alloys in Chapter 6).

The bond-by-bond method is convenient for many purposes because we can consider any nth neighbor interaction between any orbital in the solid and any other as long as we can calculate appropriate g and E terms for insertion into the matrix of Equation 5.14. Standard methods for calculation of such parameters exist. In addition, we can easily add shallow-lying d-orbitals or other states that are not part of the normal sp^3 orbital geometry to the bonding. This is essential to an exact description of bonding in compound semiconductors involving elements below row three in the periodic table. When the d-orbital has a high binding energy, its wave function decays fast enough that it does not contribute significantly to bonding. However, the group IIb and IIIb metals such as Zn and Ga include d-orbitals shallow enough to be important. In some of the largest elements even f-states may contribute measurably (for example in HfN). Likewise, it is the second-nearest-neighbor atomic orbital interactions that distinguish between fcc and hcp crystal structures. Such interactions are small and change with the atomic number of the atoms involved. This explains why cubic and hexagonal forms may coexist in compounds such as ZnS or GaN and why one sees a transition from a stable cubic form to a stable hexagonal form with position of the constituent elements in the periodic table.

Table 5.3: **Energy Gaps and Lattice Parameters**

Semiconductor Class	Semiconductor	Lattice Parameter	Energy Gap, eV (at 20°C)	E_c (eV)	E_v (eV)
Cubic		nm			
IV	C (diamond)	0.35597	5.5		
IV	Si	0.54307	1.12 (indirect)	4.05	5.17
IV	Ge	0.56754	0.67 (indirect)	4.0	4.67
IV	a-Sn	0.64912	0.08		
III-V	GaP	0.54505	2.26 (indirect)	3.8	6.1
III-V	GaAs	0.56532	1.42	4.07	5.49
III-V	GaSb	0.609593	0.726	4.06	4.79
III-V	InP	0.58687	1.344	4.38	5.72
III-V	InAs	0.60583	0.354	4.9	5.25
III-V	InSb	0.6479	0.17	4.59	4.76
II-VI	ZnSe (cubic)	0.567	2.58	4.1	6.7
I-VII	CuBr	5.69	2.94	4.35	7.29
I-III-VI_2	$CuInSe_2$	0.578	0.98	4.0	5.0
II-IV-V_2	$ZnGeAs_2$	0.567	0.85		
Hexagonal					
III-V	AlN	0.3111 (a) 0.4978 (c)	5.9	0.6	6.5
III-V	GaN	0.3190 (a) 0.5189 (c)	3.45	4.0	7.4
III-V	InN	0.3533 (a) 0.5693 (c)	0.7 (note values vary greatly)		
II-VI	ZnS	0.3814 (a) 0.6258 (c)	3.911		
II-VI	CdSe	0.4299 (a) 0.7010 (c)	1.751 eV		
E_c (the electron affinity) and E_v (electron affinity + energy gap) measured with respect to the vacuum level. Lattice parameters in nm.					

5.3 COMMON SEMICONDUCTOR ENERGY BANDS

Having armed ourselves with a more detailed idea of how energy bands develop in semiconductors, we now consider some specific examples. It is helpful to begin with an examination of some experimental data for some representative semiconductors. Table 5.3 lists lattice parameters and energy gaps for selected common semiconductors. Several of the trends listed above are illustrated by these results.

For the group IV semiconductors the effect of the homopolar splitting on energy gap and its dependence on lattice constant are shown in Figure 5.7. Complete band

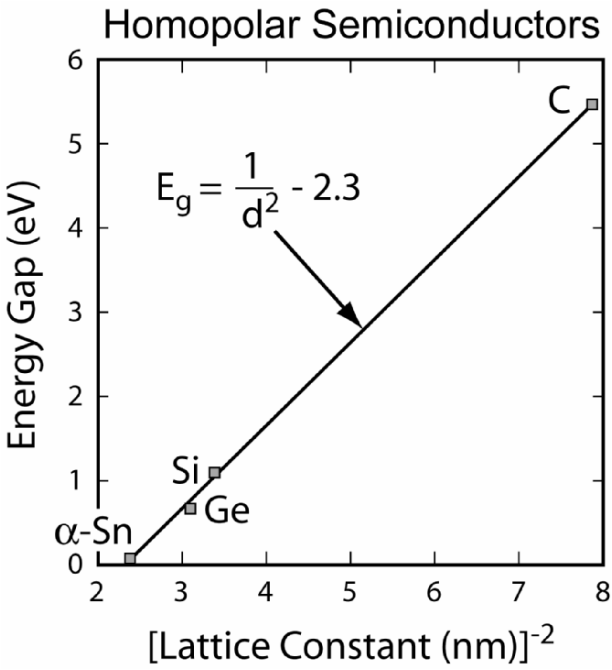

Figure 5.7: Shows the relationship of minimum energy gap to lattice constant for the common diamond-structure semiconductors.

structures will be discussed later in the section. The results range from diamond with the smallest lattice constant and largest gap to α-Sn with the largest lattice constant and smallest gap. The behavior fits well with a change in energy gap proportional to the inverse square of the lattice constant, as would be expected from Equation 5.3. The observation might be surprising as two of the materials have indirect gaps with minima at different symmetry points while the other two have direct gaps. Therefore, the detailed trends might not be expected to be as anticipated from Equation 5.3. Nonetheless, the general scaling behavior of the potentials is clear.

The situation is less surprising when one considers that the bonding-antibonding splitting has much more effect on the energy gap than do the details of the energy bands. As we found via Equation 5.18, bond-length-induced changes in the bonding-antibonding splitting have a much larger magnitude than do the changes in band-width. It is interesting to note that such an obvious trend in homopolar splitting is hard to observe in compound semiconductors because of the simultaneous change in chemical splitting. For example, the sequence BN, AlP, GaAs, InSb could, in principle, show a dominant effect of homopolar splitting. Certainly the lattice

parameter changes are sufficient to expect a large change in homopolar splitting. However, the chemical changes in this sequence turn out to dominate the results, as might have been anticipated from Equation 5.8.

A comparison showing the effect of chemical splitting can be obtained most clearly based on the row-four semiconductors Ge, GaAs, ZnSe, and CuBr. The lattice constants in these materials are almost identical and all are cubic. Therefore, virtually all of the difference in their bands is the result of the chemical changes. The trend here is not as clear as in Figure 5.7 for the homopolar materials but for Ge, GaAs, and CuBr the results are still in good agreement with the relationship of chemical splitting to energy gap. A plot comparing the minimum energy gap in these materials with the bonding/antibonding splitting estimated using Equation 5.7 is given in Figure 5.8.

The general trends for chemical and homopolar splitting appear to be borne out by the behaviors of the minimum energy gaps in most cases. Let us now consider the complete band structures and look for additional trends there. The energy band structures for six semiconductors calculated by an enhanced LCAO method [5] are shown in Figures 5.9 (the series of group IV diamond structure materials Si, Ge, and α-Sn) and 5.10 (the fourth row series Ge, GaAs, and ZnSe).

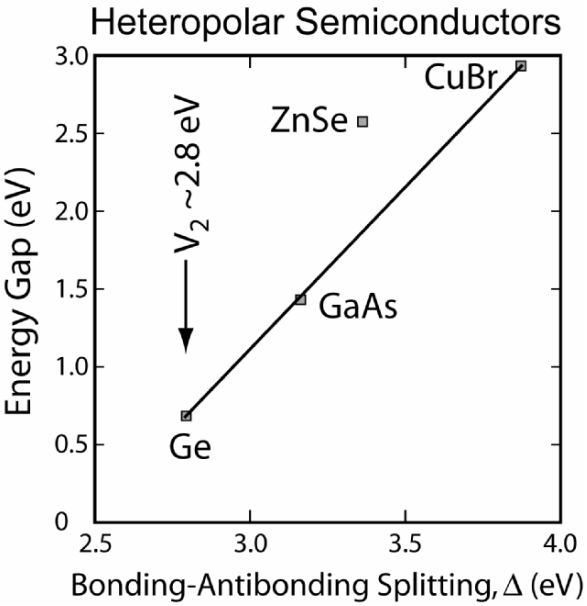

Figure 5.8: Changes in the energy gap of heteropolar semiconductors made up from elements in row 4 of the periodic table showing the effect of chemical splitting on the energy gap. Values used in generating this figure are from Table 5.2.

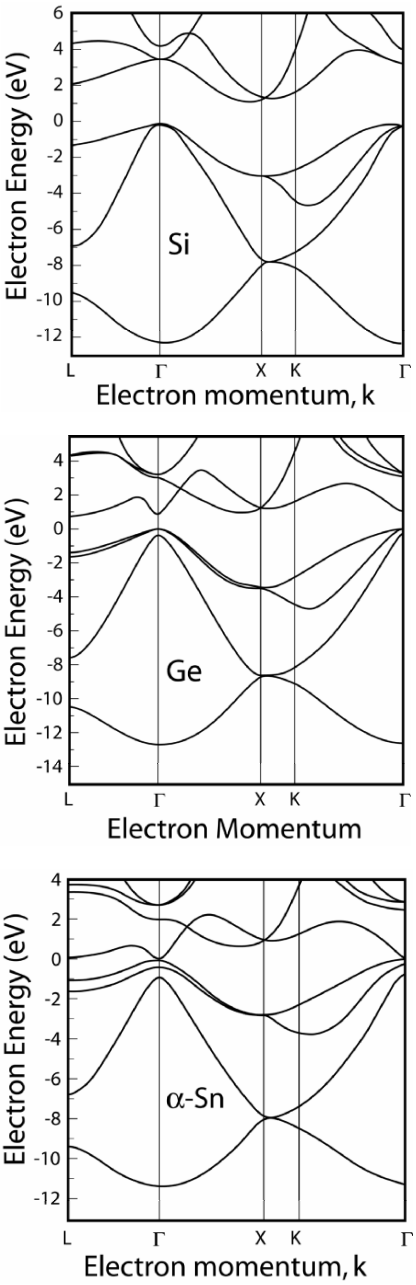

Figure 5.9: Energy band structures for the Group IV semiconductors Si, Ge, and Sn. Redrawn with permission from Chelikowski, J.R. and Cohen M.L. *Phys. Rev. B* **14**, 556-582 (1976). Copyright 1976, American Physical Society.

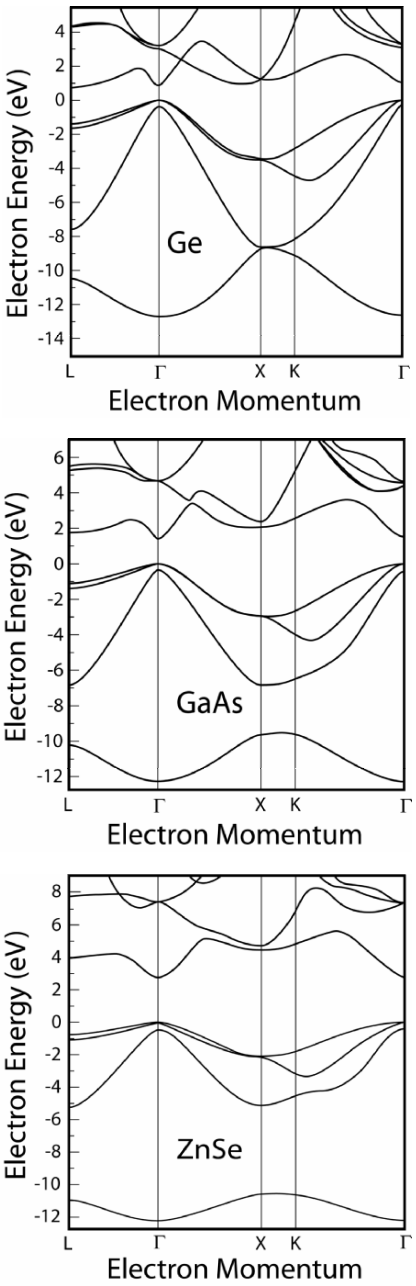

Figure 5.10: Energy band structures for the row 4 semiconductors Ge, GaAs, and ZnSe. Redrawn with permission from Chelikowski, J.R. and Cohen M.L. *Phys. Rev. B* **14**, 556-582 (1976). Copyright 1976, American Physical Society.

Details of the calculation and discussion of the band structures may be found in the original paper in which these results were presented by Chelikowski and Cohen [5].

There are several significant trends to notice about the band structures in Figures 5.9 and 5.10. For example, the homopolar group IV series, taking a vertical slice through the periodic table, shows very similar band structures. The most obvious change is that the conduction band minimum moves downward in energy relative to the top of the valence band, consistent with the reduction in bonding-antibonding splitting (V_2) as the bonds lengthen. More interesting are the relative behaviors at the Γ, X, and L points with bond length. The Γ point energy at the conduction band minimum shifts by more than 4 eV from Si to α-Sn, while the L point shifts by less than half of this energy and the X valley hardly shifts at all. Thus, some regions of the bands are much more sensitive to bond length than others. The large change at Γ and relatively small changes at X and L suggest that the sp σ-bonds and p-p π-interactions are becoming less significant as Z increases by comparison with the s-s and p-p σ-bonds. The p-p π-bonds turn out to primarily affect the width of the bands (or the dispersion with respect to **k**). The most significant change in the valence band as Z increases is the increased splitting among the p-states, primarily near the top of the band. This is due to increased spin-orbit interaction in higher Z elements. In addition, there is a modest change in valence bandwidth, resulting from the reduction in orbital overlap as the interatomic distance increases.

One can equally well consider a series of analogous heteropolar semiconductors moving down the periodic table; for example, by comparing AlP, GaAs, and InSb or ZnSe, and CdTe. Such comparisons show nearly the same trends with increasing Z as in homopolar semiconductors – the energy gap shrinks but the general features of the valence and conduction bands remain virtually unchanged. A notable difference is that by comparison to the homopolar materials there is even less change in the conduction bands. This is because the more ionic nature of heteropolar materials softens directionality and atomic orbital energies dominate over directional terms such as E_{xy}. Only in the smallest compounds such as AlP does one find indirect energy gaps in these materials and then only occasionally.

The situation as one follows a series of increasingly ionic compounds within a given row, Figure 5.10, is much different. As expected from Equation 5.7 and Figure 5.8, the energy gap increases with increasing chemical splitting. In addition, the valence bands change very obviously with the energies between the top and bottom of states due to a particular interaction (the band dispersion) decreasing as the atoms move apart in the periodic table. For example, while the p-like and s-like portions of the valence bands remain centered around roughly constant energies, the width of these parts of the valence band shrink. This causes a gap to open within the band.

The decreasing variation in energy with momentum across the diagram is not, perhaps, very surprising given the discussion in Section 5.1. As the chemical splitting increases, the bonds become increasingly ionic. **Ionic bonds are relatively**

non-directional and localized on a specific atom. A purely ionic bond results from electrostatic interactions, which are spherically symmetric (no dispersion with direction). Consequently, the bands become narrower as a function of **k** for increasing ionicity as direction becomes increasingly unimportant. The s-like portion of the valence band that merged with the p-like valence band in group-IV compounds (the bottom band in the -8 to -12 eV energy range) separates increasingly from the rest of the valence band as the polarity of the compound increases. Bands that crossed in the conduction band without interacting in the elemental semiconductor Ge react increasingly strongly in the less symmetric compound materials. As polarity of the materials increases the breadth of features in momentum space also changes with consequences for the effective mass of electrons and holes.

Unlike the homopolar materials that showed relatively dramatic changes in the conduction band as the atoms increase in Z, the heteropolar materials with fixed average Z show very similar conduction band behaviors. Note that the lower dispersion in ionic compounds results, among other effects, in these materials having direct energy gaps. It is nearly impossible for a highly ionic compound to have an indirect energy gap because the ionic bonds are much less directional than are covalent bonds. Consequently, the distinction between directions is smaller and it is less likely that a non-zero momentum wave vector will have a lower energy than for the zero-momentum Γ point. Indirect gaps are also absent from amorphous materials. In this case it is for the simple reason that specific directions do not exist.

An instructive alternative approach to visualizing the bonding and electron distribution in semiconductors is to construct a map of constant electron density surfaces in the material. An example of such a map for the electron density on a (110) plane of GaAs, along with the corresponding crystal lattice, is shown schematically in Figure 5.11. Similar maps can be constructed for slices through other atomic planes with different symmetries [see the original work by Chelikowski and Cohen, Ref. 5, for examples]. A sketch of the sp^3 hybrid orbitals for the anion (As in this case) is overlain on the diagram to show that the regions of high contour density correspond to the primary bond directions. Note that this is a plot of the electron density. Therefore, it corresponds to the amplitude of the wave functions of the valence band for various positions and hence reflects the symmetry of the valence band.

We can then compare such maps for different semiconductors. The electron density maps for the semiconductors for which the band diagrams are given in Figures 5.9 and 5.10 are shown in Figure 5.12. [5] One can see from a comparison of these diagrams that the electron density maps of the homopolar semiconductors are almost identical (the Si contour spacing is half that of the other diagrams). In heteropolar materials, by contrast, increasing the chemical splitting leads to increasing electron density around the anion and a corresponding decrease around the cation. Note that the diagrams in Figure 5.12 are for the valence band (filled states). Thus, the contours are enhanced around the anion because it makes a greater contribution to

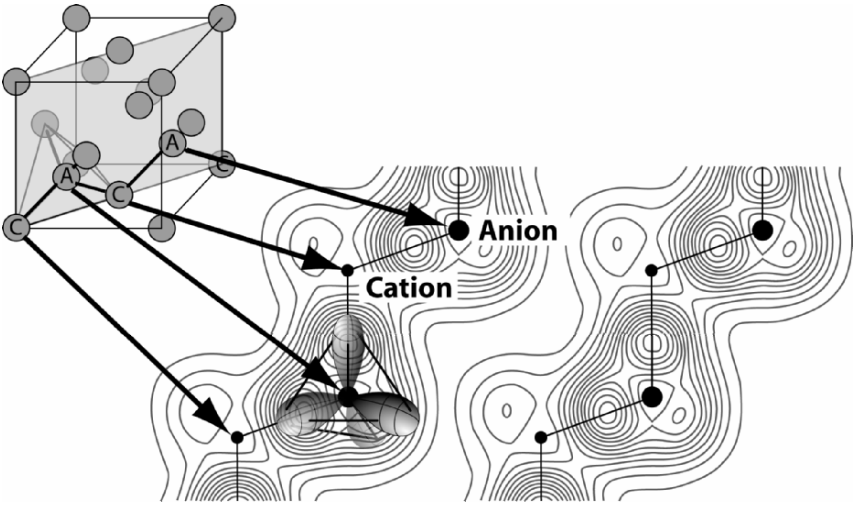

Figure 5.11: Shows a schematic diagram of the (110) plane in a zincblende-structure lattice with atoms marked C and A for cation and anion sites, respectively. The corresponding electron density map in this plane for GaAs is given as well based on the calculations of Chelikowski and Cohen. [5] The sp^3 hybrid orbitals of the anion are superimposed on a portion of the map to show the orientation of the orbitals. Two of the orbitals lie in the plane of the figure and two fall above or below the plane of the map. Note in particular the difference in electron density on the Ga compared to the As.

the valence band and acquires more electron density because of the ionic nature of the bond. A plot of the states in the conduction bands would be generally a complement of the valence bands and would be centered more strongly around the cation. Therefore, the symmetry of the states in the conduction band would vary more from material to material, especially for the homopolar materials. Concerning directionality of the bonding, note how much more spherically-symmetric the electron density becomes for ZnSe at the midpoint between the Zn and the Se atoms as compared to the same electron densities for GaAs and Ge. The much larger variation of electron density with angle for the smaller atoms is a reflection of the greater dispersion with angle in the energy band diagrams.

Summarizing the main trends:

- Materials with larger lattice constants have smaller energy gaps and less dispersion in their bands of states.
- Compounds involving atoms chosen from similar columns in the periodic table (group IV, III-V, II-VI etc…) have similar band structures.
- Compounds involving increasingly ionic bonds have less dispersion in their bands across momentum space (the E(k) diagrams).

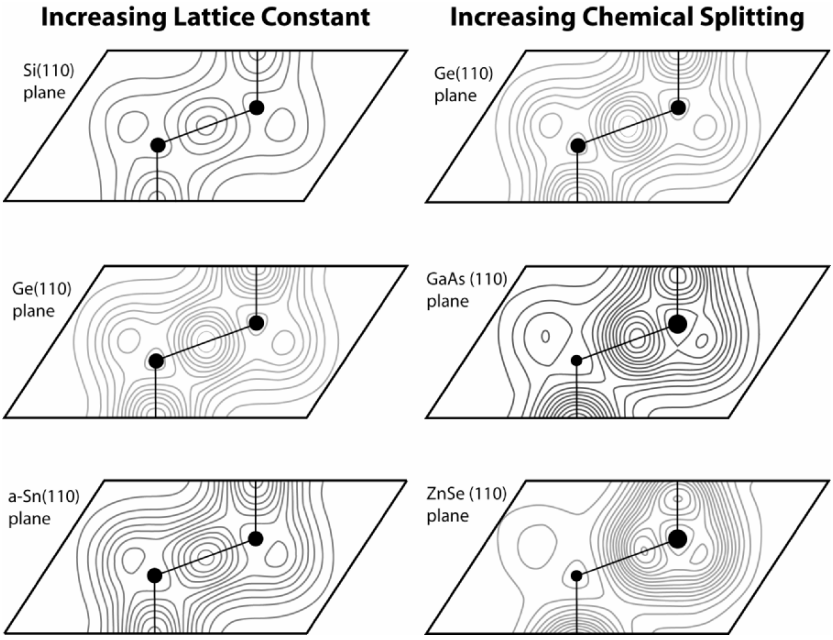

Figure 5.12: Electron density maps for a series of homopolar semiconductors of different lattice size showing the effect (or lack thereof) of lattice constant on electron density. Also shown is a corresponding series for increasingly ionic semiconductor compounds in row four of the periodic table. Contours for Si are at half the spacing of the other homopolar materials. Redrawn with permission from Chelikowski, J.R. and Cohen M.L. *Phys. Rev. B* **14**, 556-582 556-582 (1976). Copyright 1976, American Physical Society.

- Indirect gap semiconductors are made up of smaller, more covalent compounds or elements.

The detailed quantum mechanical basis for all of these changes is discussed in great detail in Harrison and many other sources but the reader is cautioned that a solid understanding of the notations of quantum mechanics is required to understand the discussion.

5.4 PRESSURE AND TEMPERATURE DEPENDENCE

We can combine many of the above points to understand the variation in the minimum direct and indirect energy gaps in semiconductors with hydrostatic pressure and temperature.

Hydrostatic pressure is uniform over the surface of a body and can be compressive or tensile. Compressive forces on an isotropic material push atoms slightly closer

together while tensile forces pull them apart. Hydrostatic pressure, P, is a force per unit area (or stress). It induces a strain, ε, in a material which is linearly related to the pressure through the Young's modulus, Y: $\Delta P = Y\Delta\varepsilon$. The strain is defined as $\varepsilon=(l_f-l_i)/l_i$, where l_f is the final length of the material and l_i is its initial length. Bond length is directly related to strain as $\varepsilon=\Delta d/d$, where d is the interatomic distance. $\Delta\varepsilon$ is the change in this strain as the stress (pressure) changes. Thus, increasing the pressure decreases the interatomic distance. As this occurs, the bonding and antibonding states draw apart as is implied by Equations 5.3 and 5.6. The band widths also increase or change shape slightly as discussed in the preceding section resulting in changes in dispersion as well as changes in the minimum direct energy gap at the Γ point. For the direct gap, as it turns out, the increase in homopolar splitting and chemical splitting win out over the increase in band width as interatomic spacing decreases, leaving a roughly linear relationship between gap and pressure over the range of pressures normally studied. Because the direct gap increases with decreasing distance, the rate of change in energy gap with pressure (dE_{gap}/dP) is positive (increasing pressure, increasing gap). Some typical values are given in Table 5.4.

Table 5.4: **Pressure and Temperature Dependences of Selected Semiconductor Minimum Energy Gaps**

Material	**E_g (300 K)**	**dE_g/dT**		**dE_g/dP (direct)**	**dE_g/dP (indirect)**
	eV	A (eV/K) $x10^4$	B (K) for Eq. 5.11	$x10^{-6}$ eV•cm^2/Kg	$x10^{-6}$ eV•cm^2/Kg
Si	1.107	2.3	636	10.5	-1.09
Ge	0.67	3.7			+7.3
GaP	1.6	5.4			-1.7
GaAs	1.35	5.4	204	11	
InP	1.27	4.6		4.6	
InSb	0.165	2.8		15	
ZnSe	2.58	7.2		6	
CdTe	1.44	4.1		8	

Si and GaAs data from Sze (1981). [6] Remaining data from the CRC Handbook of Chemical Physics, 2001. [3] When no value is given it may be assumed that B<<300K.

The relationship between energy gap and pressure is different for indirect gap materials. In these there is, necessarily, a strong dispersion in the conduction band. This is essential to get a high-momentum part of the energy band below the zero-momentum minimum and explains why relatively ionic semiconductors have direct energy gaps. As Figure 5.7 shows, smaller interatomic distances lead to larger conduction band dispersions, strongly increasing the Γ-point energy and simultaneously reducing the energy of other points in the energy bands. This suggests that the behavior of the energy gap with pressure should be different and, indeed, opposite

away from Γ; which is what is observed for most materials (Ge is an exception). Thus, in many indirect-gap semiconductors dE/dP < 0, indicating that as pressure increases, the gap decreases and becomes more indirect (see Table 5.4).

Theoretically, the opposite dependence of direct and indirect gaps on pressure could be used to convert indirect gap materials to direct gaps. However, a negative pressure (tensile stress) would have to be applied to achieve this conversion. Ceramics, including semiconductors, tend to be weaker in tension than in compression. Even by placing the indirect material in a strained-layer superlattice (see Chapter 7), which can achieve the highest tensile stress levels, it has been impossible to convert indirect semiconductors to direct gaps before the stress is relieved by formation of dislocations or by fracture.

The link between lattice constant and temperature also results in a change in energy gap. The quantitative relationship is less clear than in the case of pressure. The most straightforward connection is through the thermal expansion coefficient of the semiconductor, leading to an increase in interatomic spacing as the temperature rises. This causes a decrease in minimum direct energy gap with increasing temperature. In addition, interaction of electrons with phonon lattice vibrations changes as the phonon density changes with temperature and affects the band structure. The change in gap with temperature at constant volume is given roughly by:

$$\left(\frac{\partial \mathrm{E}_{\mathrm{gap}}}{\partial \mathrm{T}}\right)_{\mathrm{V}} = -3\alpha \mathrm{G}\left(\frac{\partial \mathrm{E}_{\mathrm{gap}}}{\partial \mathrm{P}}\right)_{\mathrm{T}} \qquad 5.19$$

where α is the thermal expansion coefficient, G is the bulk modulus, and $\partial E_{gap}/dP$ is the pressure dependence of the energy gap, discussed above. More typically, an empirical relationship between temperature and lattice parameter is observed:

$$E_{gap}(T) = E_{gap}(T=0) - \frac{AT^2}{T+B}, \qquad 5.20$$

where A and B are constants. In other words, the gap depends quadratically on temperature at low temperatures and linearly on temperature at high temperature. Data for A (and B when available) in Equation 5.20 for several common semiconductors are given in Table 5.4. Values without a corresponding B show a linear change in gap with temperature. The linear behavior can be obtained directly from Equation 5.19, assuming a constant relationship of energy gap to pressure. In addition to broadening of the energy gap with decreasing T, structures in the density of states and features of the band structure also broaden.

5.5 APPLICATIONS

5.5.1 Experimental band structures

Direct application of the material in this chapter relates more to fundamental understanding of why semiconductors are the way they are than directly to making most semiconductor devices. Thus, one practical application for this chapter is in the interpretation of ultraviolet photoelectron spectroscopy (UPS) results. One can equally well view UPS as a way of measuring the band structures experimentally. It is UPS data which one generally fits to obtain, for example, an accurate E(k) diagram. We will begin this section by considering the UPS and inverse photoemission processes and how they can measure band structures directly. The experiments demonstrate that band structures are not hypothetical objects but real observables. The apparatus and electronic transitions in a solid associated with UPS photoemission are shown schematically in Figure 5.13.

To obtain valence band structure of a solid by normal photoemission, one arranges the experiment as follows. A linearly polarized photon strikes a smooth single crystal surface, ideally as free of defect states as possible, in a direction that is well defined with respect to the crystal lattice. This requires the ability to precisely tilt and rotate the crystal through a range of angles with respect to the incident photons. Both tilt with respect to the photon source and rotation in the surface plane are generally needed. It is helpful to be able to change the angle between the source and the detector. Because the photon is polarized and incident along a well controlled crystal direction, its wave vector is well defined. A similar ability to orient a detector relative to the crystal allows the momentum direction of emitted electrons to be determined. Finally, an energy analyzer is incorporated into the detector from which the photoelectron kinetic energy is determined. The energy of the state from which the electron originated relative to vacuum is then the difference between the energy of the photon and the vacuum level energy. For absorption of the photon and emission of the electron, the total momentum and energy are conserved. Consequently, the initial momentum and energy of the electron in the solid can be determined. Thus, measurements of photoelectron energies as a function of take-off angle give a measure of the band structure.

Inverse photoemission measures the conduction band states in a similar manner. In this case, an energetic electron beam strikes the solid from a fixed direction and with a fixed energy (thereby defining both the initial energy and momentum). The electron may be captured by the solid into a single unoccupied state with a consequent need to release the excess energy of the incident electron plus the binding energy of the state. Sometimes this energy is released by photon emission. Detection of the emitted photons in a given direction allows determination of their energy. From these pieces of information the energy and momentum of the electron in the bound state may be determined as for conventional photoemission.

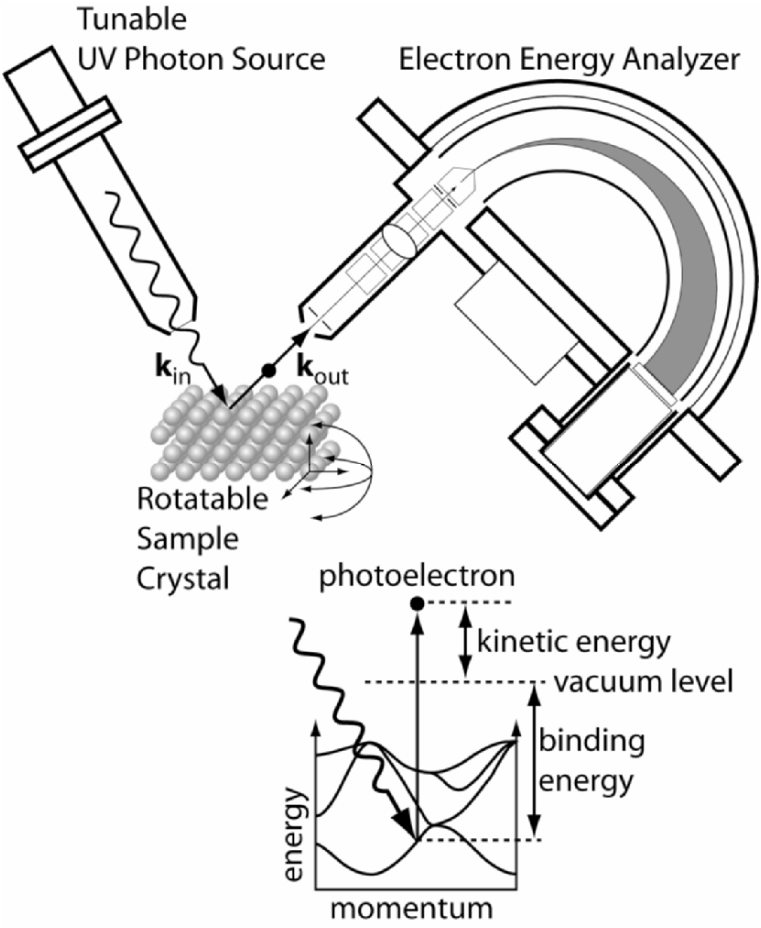

Figure 5.13: A schematic diagram of the photoemission process used to determine the structure of the valence band as a function of electron wavevector, **k**. The incident photon has a well-defined momentum $\mathbf{k}_{in}$ and the photoelectron has an outgoing wave vector $\mathbf{k}_{out}$. For an energy and momentum conserving process the initial energy and momentum of the electron can be determined, from which the band energy is known.

Typical experimental results for the valence and conduction bands of GaAs are shown in Figure 5.14 [7]. Not all values of incident and outgoing momentum can be probed effectively with a given apparatus. Furthermore, there may be portions of the energy-momentum space where it is too difficult to separate components of the band

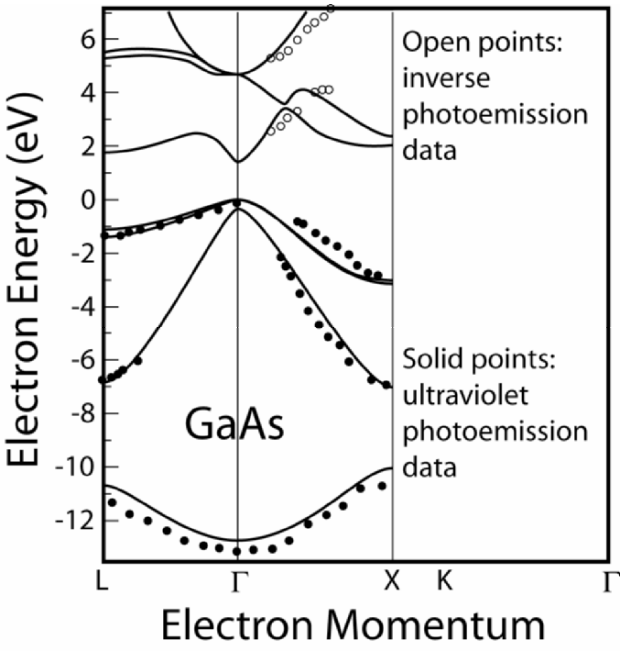

Figure 5.14: Experimental determination of a portion of the GaAs band structure as a function of electron momentum (points) by Ortega and Himpsel. [7] Also the calculation by Chelikowski and Cohen [5] (curves) for the band structure of GaAs. The agreement is excellent for the valence band and generally good for the conduction band. Adapted with permission from Ortega, J.E. and Himpsel, F.J. *Phys. Rev. B* **47**, 2130-7 (1993). Copyright 1993 by the American Physical Society.

structure in the output data. However, as the data in Figure 5.14 shows, it is possible to obtain very good experimental agreement with theory with some effort.

5.5.2 Gunn diodes

One can see a direct application of the concepts in this chapter in some more unusual electronic devices. An example is the Gunn effect, and resulting Gunn diodes, which have been used to produce high-frequency oscillators. In most semiconductors, as electrons accelerate they scatter increasingly strongly off the lattice, generating phonons and decelerating the electron. It is found that the carrier mobility becomes limited in proportion to the inverse of the electric field in the material [see, for example the discussion in Hess]. Consequently, a higher field produces a lower mobility. If we recall that the electron current density in the material is $J_e = q\mu_n n\mathcal{E}$ (Equation 3.6), then we see immediately that if μ_n is inversely proportional to $\mathcal{E}$ then J is independent of electric field.

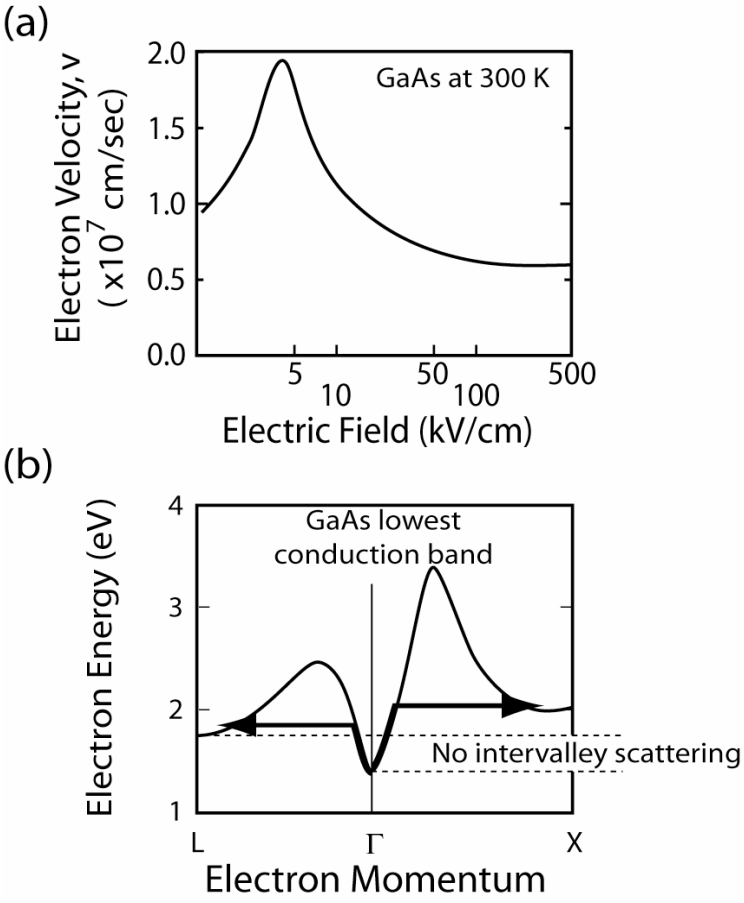

Figure 5.15: (a) Calculated carrier velocities in pure GaAs at 300 K as a function of electric field and (b) a schematic diagram of the lowest branch of the conduction band. Arrows indicate the acceleration and scattering of carriers to the X and L minima. At low energies no scattering is possible because states are only available around the Γ point. Once one reaches the energy of other band minima scattering begins and the carrier velocity starts to decrease. Part (a) redrawn with permission from Shichijo, H. and Hess, K. *Phys. Rev. B* **23**, 4197-4207 (1981). Copyright 1981 by the American Physical Society.

In other words, the electron velocity saturates. However, in semiconductors such as GaAs that have a low effective electron mass and modest phonon scattering rate, carriers may accelerate to relatively high velocities. The predominant scattering process becomes inter-valley scattering, rather than phonon emission within the same valley. In GaAs the scattering occurs to the X and L valleys as shown schematically in Figure 5.15. Electrons in these regions of the band structure have much higher

effective mass (see Section 2.1.7 and Equation 2.18). Consequently, at the same energy they travel much more slowly.

The number of electrons in the high-mass valleys increases as the electric field increases because at higher fields electrons in the low-momentum valley near Γ accelerate very fast to a point where scattering to the other valleys is rapid. The consequence of this behavior is that the electron velocity has a maximum at a given field (see Figure 5.15) and decreases above and below this value. For a decrease in velocity to occur at constant (or increasing) electric field, the mobility must decrease, as one would expect if the effective mass increases. The resistance of the device is inversely related to the mobility.

When the resistance increases as voltage increases it produces a negative differential resistance in the device. In other words, the current voltage curve has a decreasing region at high voltage. Any time a device has a negative differential resistance an electronic circuit incorporating it is unstable and will switch between different operating points. The current/voltage curve for such a device is shown in Figure 5.16 with the unstable operating region marked. When the device is biased to a voltage in the unstable region it switches from one stable operating point to another at a given voltage or current. In short, it oscillates. Such an oscillation makes sense, perhaps, based on the following argument.

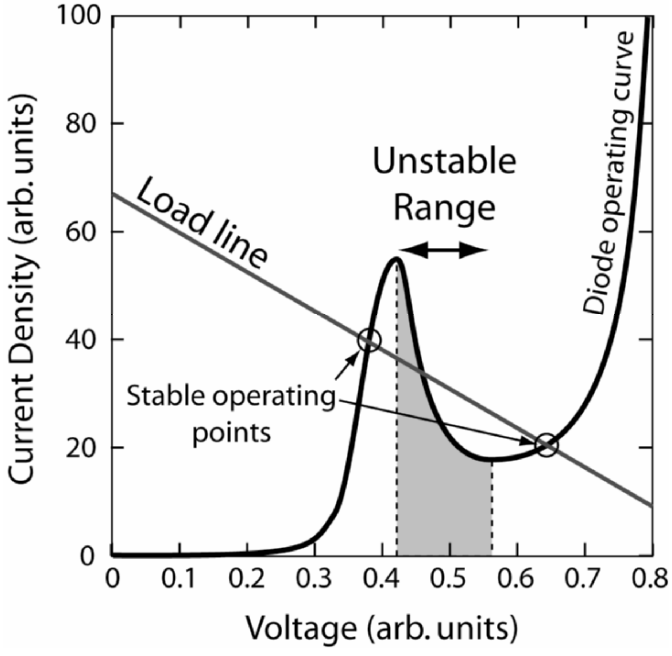

Figure 5.16: A schematic diagram of the current voltage curve for a Gunn diode. The device will not operate in a stable mode anywhere in the negative resistance region as marked. For the load line indicated the circuit has two stable operating points as shown.

At any point in the device where a local fluctuation in resistance raises the field in that region (higher resistance), scattering increases, mobility decreases, and resistance rises further in that area. This produces a local volume where a large fraction of the applied field is dropped. In this region, mobility decreases and velocity saturates. Carriers in low-resistance regions of the device continue to move well as the field is low. Although the carrier velocity is relatively low compared to the peak level in the high-field area, it is still of the order of the thermal velocity ($\sim 1 \times 10^7$ cm s^{-1}). Consequently the high field pocket can drift in the device in the direction of the positive contact. When it reaches the positive contact it disappears. As long as it is short enough, the device oscillates as high-resistance pockets form near the negative contact, drift to the positive contact, and are eliminated. The resulting circuit typically shows microwave oscillations.

So far, the description of the Gunn effect does not make use of designed materials. One could imagine that any direct-gap semiconductor with a sharp minimum at Γ and a broad minimum at some other momentum would suffice. However, we may wish to control the relative energies of the two minima such that a given amount of acceleration would occur before the onset of scattering. Such control can easily be obtained by either application of pressure, which allows adjustment of the relative energies of the direct and indirect gap minima, or, more practically, by alloying a direct gap material with an indirect gap material such that the appropriate energy difference between the direct and indirect gap minima would be obtained. Methods for band-gap engineering are discussed in detail in the next chapter where semiconductor alloys are described in detail. Note however that alloys typically have much lower carrier mobilities than pure compounds so the devices may function better with a strained layer than with an alloy.

5.6 SUMMARY POINTS

- Homopolar semiconductors consist of a single type of atoms.
- Heteropolar semiconductors consist of multiple atoms.
- Molecular orbitals are linear combinations of atomic orbitals.
- Symmetric combinations of atomic or molecular orbitals produce bonding states
- Antisymmetric combinations produce antibonding states.
- Homopolar splittings are the differences between bonding and antibonding state energies in the absence of chemical differences between atoms. The homopolar splitting varies inversely as the square of the interatomic distance. All other aspects of homopolar bonding, including the energy gap, tend to scale as $1/d^2$.
- Heteropolar compounds have both chemical and homopolar splittings contributing to their band structure and bond energy.
- Increasing chemical differences between atoms in heteropolar compounds lead to more ionic bonds, to an increasing connection of the valence band with the anion, and the conduction band with the cation. This is the basis of the common cation and common anion rules.
- Bonding can be treated as interactions of all individual atomic orbitals with all others as represented by the eigenvalues of the matrix of Equation 5.13. The matrix elements are affected by the electron wave vectors, the location of atoms contributing orbitals, and the energy of atomic orbitals and their interactions.
- The top of the valence band in common semiconductors is primarily derived from p-like states and has three branches resulting from the three p-orbitals. The bottom of the conduction band is s-like.
- The matrix elements related to orbital overlaps increase approximately as $1/d^2$.
- Materials with larger lattice constants have smaller energy gaps and less dispersion in their bands of states.
- Compounds involving atoms chosen from similar columns in the periodic table (group IV, III-V, II-VI etc…) have similar band structures.
- Compounds involving increasingly ionic bonds have less dispersion in their bands across momentum space (the E(k) diagrams).
- Indirect gap semiconductors are made up of smaller, more covalent compounds or elements.
- Increasing temperature causes thermal expansion of a material, increasing interatomic distances, and hence decreases energy gap.
- Increasing pressure decreases interatomic distance and hence increases energy gap.

5.7 HOMEWORK

1) Given the formulas for the s and p atomic orbitals in Figure 5.1, plot contours of constant wave function intensity in the r – theta plane.

2) Given the formulas for the p atomic orbital in Figure 5.1 and assuming that the p_y orbital is the same as the p_x but with $\sin\theta$ replacing $\cos\theta$, what is the sum of the squares of the p_x and p_y orbitals.

3) Suppose that a hypothetical homopolar semiconductor existed with a lattice constant of 0.4472 nm. Estimate its minimum energy gap. Explain briefly how you obtain this value.

4) In the energy-momentum diagram for ZnSe there is a narrow band of states between ~11 eV and 12 eV binding energies. For Ge, a similar band is found between ~ –9.5 and –13 eV. What is the atomic orbital most responsible for this band of states and why is the band narrower in ZnSe than in Ge?

5) What is the physical basis in bonding theory as described in this chapter for the common cation and common anion rules? Would you expect these rules to be more obvious when comparing GaP with GaAs or comparing CdS with CdTe? Explain briefly.

6) Equation 5.11 provides the combinations of atomic orbitals that make up the four sp^3 molecular orbitals. Write a similar set of equations for the sp^2 molecular hybrids shown in Figure 5.2.

7) Sketch a Harrison diagram similar to that of Figure 5.5, as close to correctly to scale as can reasonably be managed, for InSb using the data from the various tables in the chapter.

8) If one assumes that the contours in Figure 5.12 represent the same change in electron density except in the case of Si where the contour interval is halved, which homopolar and which heteropolar semiconductor has the stronger bonds? How do you know this to be the case and how would you connect the answer to the corresponding value of Δ for that semiconductor?

9) From the values listed in Table 5.4, calculate the hydrostatic pressure necessary to convert Si to a direct energy gap material (i.e. where the direct and indirect gaps are equal). Assume that the minimum indirect energy gap is 1.1 eV and the minimum direct gap is 3.3 eV at zero pressure.

10) Calculate and plot the values for bond polarization (α) for the series of semiconductors Ge, GaAs, ZnSe, CuBr. From these values, determine the values for u_1 and u_2 for each material.

11) Given that:

$V_{ss\sigma} = -1.40\ \hbar^2/md^2$
$V_{sp\sigma} = 1.84\ \hbar^2/md^2$
$V_{pp\sigma} = 3.24\ \hbar^2/md^2$
$V_{pp\pi} = -0.81\ \hbar^2/md^2$

Estimate the following values for GaAs using the formulas and data above and that $\hbar^2/m = 0.762$ eV-nm, and $d = a/\sqrt{3}$, where a is the lattice constant of the material:

a) The cohesive energy of GaAs
b) The four energies of the simple bands of GaAs at Γ
c) The minimum direct energy gap of GaAs
d) Compare the minimum direct gap estimated from these values to the correct value at zero Kelvin of 1.53 eV.
e) Compare the band energies calculated with those for the complete band structure for GaAs shown in Figure 5.10.

12) Could you use the Bloch wave sums in Equation 5.13 to simulate a hexagonal (wurtzite) semiconductor and distinguish the result from the corresponding cubic (zincblende) calculation? Explain why or why not.

13) Construct a version of Equation 5.13 that takes into account second-nearest neighbors.

14) Which semiconductor would make a better Gunn diode, ZnSe or GaAs? Explain briefly.

5.8 SUGGESTED READINGS & REFERENCES

Suggested Readings:

Ashcroft, Neil W. and N. Mermin, David *Solid State Physics.* Philadelphia PA: Saunders College, 1976.

David K. Ferry, *Semiconductors.* New York: Macmillan, 1991.

Harrison, Walter A. *Electronic Structure and the Properties of Solids: The Physics of the Chemical Bond.* San Francisco: Freeman, 1980.

Hess, Karl, *Advanced Theory of Semiconductor Devices*, Englewood Cliffs, NJ: Prentice Hall, 1988.

Van Vechten, J.A., "A Simple Man's View of the Thermochemistry of Semiconductors" in *Handbook on Semiconductors*, ed. T.S. Moss, Vol. 3, *Materials, Properties, and Preparation*, ed. S.P. Keller, North Holland, Amsterdam, 1980, Chapter 1.

References:

[1] Harrison, Walter A. *Electronic Structure and the Properties of Solids: The Physics of the Chemical Bond.* San Francisco: Freeman, 1980.

[2] Ferry, David K. *Semiconductors* New York: Macmillan, 1991.

[3] Lide, David R., editor, *CRC Handbook of Chemistry and Physics*. Boca Raton, FL: Chapman and Hall/CRC, 2001; also available on line at http://www.hbcpnetbase.com/.

[4] Chadi, D.J. and Cohen, M.L. "Tight binding calculations of the valence bands of diamond and zincblende crystals." *Physica Status Solidi B*, 1975; 68: 405-19.

[5] Chelikowsky, J.R. and Cohen, M.L. "Nonlocal pseudopotential calculations for the electronic structure of eleven diamond and zinc-blende semiconductors." *Phys. Rev. B,* 1976; 14**:** 556-582.

[6] Sze, S.M. *Physics of Semiconductor Devices*. New York: Wiley, 1981.

[7] Ortega, J.E., and Himpsel, F.J. "Inverse-photoemission study of Ge(100), Si(100), and GaAs(100): bulk bands and surface states." *Phys. Rev. B,* 1993; 47(4): 2130-7.

[8] Shichijo, H, and Hess, K. "Band structure-dependent transport and impact ionization in GaAs." *Phys. Rev. B,* 1981; 23: 4197-4207.